Invariant timescale hierarchy across the cortical somatosensory network

Román Rossi-Pool[a,1] , Antonio Zainos[a] , Manuel Alvarez[a], Sergio Parra[a] , Jerónimo Zizumbo[a] , and Ranulfo Romo[a,1,2]

[a]Instituto de Fisiología Celular–Neurociencias, Universidad Nacional Autónoma de México, 04510 Mexico City, Mexico

The ability of cortical networks to integrate information from different sources is essential for cognitive processes. On one hand, sensory areas exhibit fast dynamics often phase-locked to stimulation; on the other hand, frontal lobe areas with slow response latencies to stimuli must integrate and maintain information for longer periods. Thus, cortical areas may require different timescales depending on their functional role. Studying the cortical somatosensory network while monkeys discriminated between two vibrotactile stimulus patterns, we found that a hierarchical order could be established across cortical areas based on their intrinsic timescales. Further, even though subareas (areas 3b, 1, and 2) of the primary somatosensory (S1) cortex exhibit analogous firing rate responses, a clear differentiation was observed in their timescales. Importantly, we observed that this inherent timescale hierarchy was invariant between task contexts (demanding vs. nondemanding). Even if task context severely affected neural coding in cortical areas downstream to S1, their timescales remained unaffected. Moreover, we found that these time constants were invariant across neurons with different latencies or coding. Although neurons had completely different dynamics, they all exhibited comparable timescales within each cortical area. Our results suggest that this measure is demonstrative of an inherent characteristic of each cortical area, is not a dynamical feature of individual neurons, and does not depend on task demands.

timescale hierarchy | behaving monkeys | somatosensory network | inherent time constants | primary somatosensory cortex

There has been an increase in compelling evidence that cortical areas are diverse not only in their coding dynamics, but also in their structural and inherent features (1). This structural heterogeneity can be viewed as an anatomic feature (2), but it may also be a critical functional feature related to higher-order cortical computations, such as sensory processing, working memory, decision making, and perception (3). For instance, these cortical heterogeneities appear to be crucial for information flow across cortices (4, 5) and for proper brain function (6, 7). If this were the case, then these inherent heterogeneities could be used to establish a hierarchy across cortices. Recently, a hierarchy was found in mice, monkeys, and humans by estimating an intrinsic time constant from the dynamics of each cortical area (8–12). Neurons from sensory cortices exhibit much faster timescales than frontal lobe neurons. Additionally, this timescale hierarchy is parallel to the hierarchical order observed for the size of spatial receptive fields across visual and somatosensory pathways (13–15). In these cases, structural heterogeneities (timescales or receptive fields) yield hierarchies that also relate to function. While neurons from early sensory cortices can be phase-locked to stimulation, neurons from downstream areas are able to associate different signals to participate in working memory, decision-making, and perceptual processes (16, 17).

Focusing on the somatosensory network, an anatomic hierarchy has been firmly established across cortical areas in primates and humans (2, 18, 19). When a stimulator moves perpendicular to the skin, cutaneous receptors are activated (20), giving rise to a signal that is conveyed by specific primary afferents to the spinal cord (21), then to the thalamus (22), and then up to the primary somatosensory cortex (S1) (13, 23). In S1, the sensory signal first arrives to area 3b (23). The next step in the somatosensory pathway is area 1. Historically, areas 3b and 1 were both considered parts of S1. Importantly, even when receptive fields increase from area 3b to area 1 (18, 24), their neuronal responses exhibit strikingly similar firing rate dynamics (13, 25, 26). This similarity makes it hard to distinguish these two areas from a coding perspective. The following cortical areas to be recruited are 2, 5, and 7b (27–29), which possess much larger receptive fields and longer response latencies but comparable phase-locking dynamics in the flutter range. The somatosensory inputs proceed to the secondary somatosensory cortex (S2), which shows a diversity of responses: ranging from pure sensory dynamics to more perceptual and categorical coding (13, 30, 31). In contrast to neurons from associative cortical areas, S2 neurons do not persistently code stimulus information during working memory periods (32). Associative areas from the frontal lobe—ventral, medial, and dorsal premotor cortices (VPC, MPC, and DPC)—and prefrontal cortex (PFC)—exhibit heterogeneous responses associated with all processes involved during somatosensory tasks: sensory coding, working memory, comparisons, and decision-making (3, 32, 33).

Significance

Cortical networks integrate information from different sources during cognitive processes. In doing so, they implement a broad diversity of time constants, constituting an organizational hierarchy. In the somatosensory network, while monkeys perform a highly demanding vibrotactile discrimination task, area 3b depicts a much faster time constant than area 1, both of which are historically included in the primary somatosensory cortex (S1). Timescales are longer in areas downstream to S1. This timescale hierarchy exhibits invariance across task context, neural coding, hemispheres, and response latency. Surprisingly, the vast heterogeneity of neural responses observed in each area is accompanied by homogeneity in timescales. Such homogeneity may be an inherent feature of each processing stage within the cortical somatosensory network.

NEUROSCIENCE

Here we used single-neuron activity recorded during a vibrotactile temporal pattern discrimination task (TPDT; Fig. 1 *A* and *B*) (34, 35) to study the inherent fluctuations during the basal period that precedes stimulus presentation. Recently, the timescale of these fluctuations was estimated with the decay of their autocorrelation (8–10, 36). We computed this autocorrelation decay across seven cortical areas that span different steps across the somatosensory network (Fig. 1*C*). Using this metric, we asked the following questions: what is the hierarchical order of these cortical areas in the somatosensory network? Further, is there any difference among the timescales of the subareas that compose S1? Additionally, we used a nondemanding variant of the TPDT as a control (light control task [LCT]), where the monkeys exhibit 100% performance (Fig. 1*B*). Coding dynamics during this control task are severely altered (34), so will autocorrelation and its suggested hierarchical order also be affected? Moreover, neurons exhibit heterogeneous coding responses in higher-order cortical areas, such as the DPC (31, 35); do timescales depend on the specific coding of neurons? In other words, in each cortical area, do the intrinsic timescales covary with the selectivity that each neuron displays, or are response selectivity and timescales independent dynamic traits?

We confirmed that a hierarchical order can be established along the cortical somatosensory network based on autocorrelation decay. Remarkably, the historical primary somatosensory cortex can be divided into at least three different timescales of temporal integration: those of areas 3b, 1, and 2. Conversely, S2 and a frontal lobe area (DPC) exhibit comparable time

constants. However, the specific autocorrelation values are much higher in the DPC. Stronger autocorrelation, which can be thought of as reverberation, may facilitate working memory in this area (17). Surprisingly, the hierarchy is preserved during the LCT. Although coding dynamics are severely affected in some areas during this nondemanding task (S2 and DPC), their autocorrelation functions are preserved. Furthermore, we separated neurons from area 1, S2, and DPC into subgroups with completely different coding and latencies. Notably, each subgroup of neurons displays a time constant comparable to its area's whole population. We also compared hemispheres and obtained similar timescales for S2 and DPC. These results show strong evidence that time constants depict a hierarchical order across the somatosensory network, which is invariant under changes of context or coding dynamics and thus are inherent to each cortical processing stage.

Results

Tasks and Datasets. Neuronal data were recorded during the TPDT. During this task, monkeys reported whether two temporal patterns composed of vibrotactile flutter stimuli (P1 and P2) were the same (P2 = P1) or different (P2 ≠ P1) (Fig. 1*A* and *SI Appendix*) (34). The stimuli presented in each trial could be one of four possible classes: G-G (c1), G-E (c2), E-G (c3), or E-E (c4). The average performance across all sessions (n_{SES} = 954) in all recorded areas was 85 ± 6%, consistently across classes (Fig. 1*B*). We recorded single neuron responses from several cortical areas involved in somatosensory processing (Fig. 1*C*): areas 3b (green), 1 (blue), 2 (pink), 5 (violet), and 7b (cyan), S2 (red), and DPC (orange).

Importantly, several neurons recorded during the TPDT were also recorded during an LCT. In trials of this control task, the animals received the same stimuli as in the TPDT, but the correct decision report was guided by a visual cue (*SI Appendix*) that was continuously present from the start of each trial (pd event in Fig. 1*A*). The TPDT and LCT were presented separately; thus, during each set of trials, the animals could expect to perform only one task. As opposed to the TPDT, the performance for LCT was consistently 100% (n_{SES} = 226; Fig. 1*B*), demonstrating that it was not cognitively demanding.

Hierarchical Timescales across the Somatosensory Network. As we stated earlier, recent studies have provided evidence that the timescale of neural fluctuations, estimated with the autocorrelation decay rate, increases across cortices based on their hierarchy (8–10, 36). However, in the somatosensory network, this has been analyzed only for S1 and S2; other relevant somatosensory cortices, in particular areas 2, 5, and 7b, have yet to be analyzed. Furthermore, S1 historically has been considered a composition of two anatomically different subareas: 3b and 1 (Fig. 1*C*). Even if receptive fields tend to increase from area 3 to area 1, firing rates are only slightly transformed between them (13, 18, 24).

To analyze the decay rate of each subarea of S1 (Fig. 2*A*), we averaged the autocorrelation across the corresponding neurons (40 ms, with steps of 20 ms), and fit an exponential function (*SI Appendix*). Note that we included area 2, which is often incorporated into S1 (24). Remarkably, a huge difference was observed between the fits obtained for each area. Notably, area 3b (τ = 35 ms) exhibited a much faster decay rate than area 1 (τ = 84 ms) and area 2 (τ = 113 ms). These empirical results show that fluctuations reverberate for a shorter period in area 3b than in area 1. Thus, area 1 is capable of integrating fluctuations with a longer time constant. Furthermore, area 2 displays even slower decay. Our results conclusively show a clear hierarchy inside S1 based on the timescale values.

Subsequently, we focused our attention on two other relevant areas from the parietal lobe involved in somatosensory processing: areas 5 and 7b (19) (Fig. 2*B*). We found that both area 5 (τ = 132 ms) and area 7b (τ = 134 ms) exhibit much longer
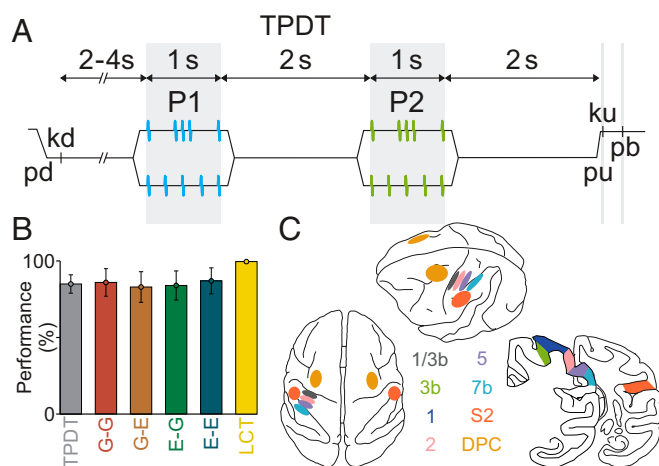

Fig. 1. TPDT, performance, and recorded cortical areas. (*A*) Trials' sequence of events. The mechanical probe is lowered (pd), indenting the glabrous skin of one fingertip of the right, restrained hand (500 μm); in response, the monkey places its left, free hand on an immovable key (kd). After a variable prestimulus period (from 2 to 4s), the probe vibrates for 1 s, generating one of two possible stimulus patterns (P1, either grouped [G] or extended [E]; mean frequency of 5 Hz). Note that in extended pattern E, pulses are delivered periodically. After a first delay (from 1 to 3 s) between P1 and P2, the second stimulus (P2) is delivered, again in either of the two possible patterns (P2, either G or E; 1 s duration); this is also called the comparison period. After a second 2-s delay (from 4 to 6 s) between the end of P2 and the probe up (pu), the monkey releases the key (ku) and presses, with its left free hand, either the lateral or the medial pushbutton (pb) to indicate whether the patterns were the same (P1 = P2) or different (P1 ≠ P2). (*B*) Performance for the whole TPDT (85%, gray; n_{SES} = 954 sessions), for each class (86% G-G [red], 83% G-E [orange], 84% E-G [green], 87% E-E [blue]) and for the entire LCT (100%, yellow; n_{SES} = 226 sessions). In the LTC, the same stimuli were delivered as in the TPDT, but the rewarding pushbutton press was visually guided. (*C*) Top (*Left*), lateral (*Middle*), and coronal (*Right*) views of the brain locations where single neurons were recorded. Cortical areas include areas 3b (green), 1 (blue), 2 (pink), 5 (violet), 7b (cyan), S2 (red), and DPC (orange). Recordings in S2 and DPC were made contralateral and ipsilateral to the stimulated fingertip.
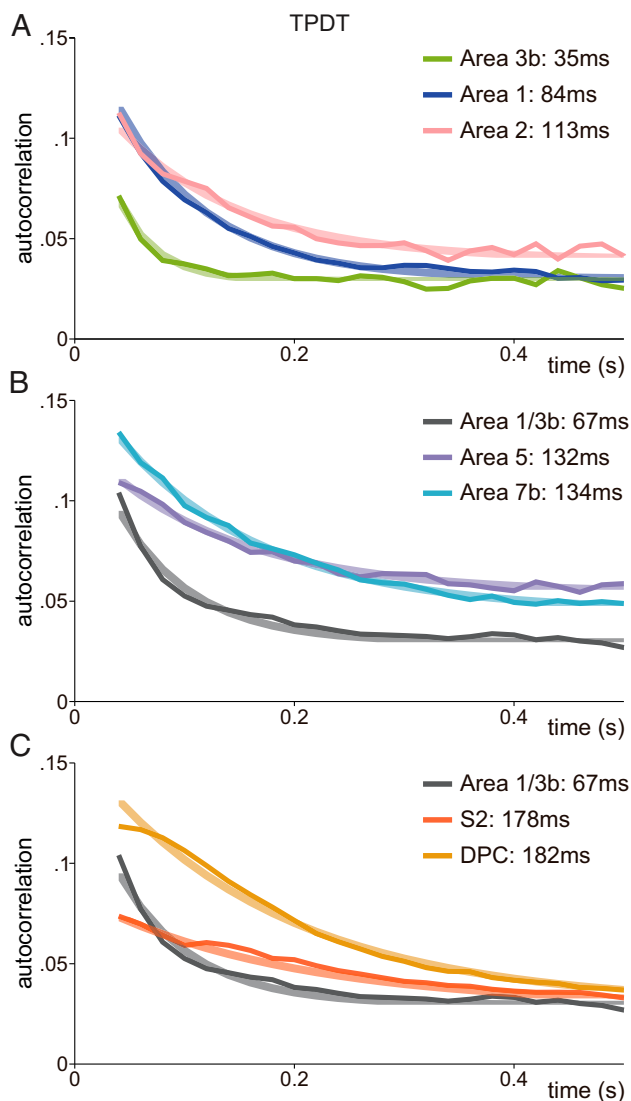
Fig. 2. Hierarchical ordering of intrinsic timescales during TPDT. The autocorrelation function was computed for neuronal activity during the TPDT basal period with 40-ms time bins. An exponential decay function was fit to the autocorrelation value (*SI Appendix*, Eq. **S1**). Confidence intervals for τ were estimated through bootstrap. Thin, darker traces show the autocorrelation values averaged across each population of neurons. Wide, lighter traces display the exponential fit for each population. (*A*) TPDT autocorrelation function for areas 3b (green; $n = 161$, $\tau = 35 \pm 11$ ms), 1 (blue; $n = 336$, $\tau = 84 \pm 13$ ms), and 2 (pink; $n = 68$, $\tau = 113 \pm 19$ ms). (*B*) Autocorrelation function for S1 (area 3b/1, gray; $n = 497$, $\tau = 67 \pm 7$ ms) compared with area 5 (violet; $n = 74$, $\tau = 132 \pm 21$ ms) and area 7b (cyan; $n = 63$, $\tau = 134 \pm 18$ ms). Neurons from areas 5 and 7b exhibit comparable autocorrelation functions but a much longer decay than S1. (*C*) TPDT autocorrelation function for the entire S1 (areas 3b and 1; gray) plotted against the S2 (red; $n = 1,646$, $\tau = 178 \pm 10$ ms) and DPC (orange; $n = 1,574$, $\tau = 182 \pm 5$ ms) populations. Note that a change of $\pm20\%$ in the time bin width for the firing rate calculation across areas (area 3b, area 1, S1 [3b and 1], area 2, area 5, area 7b, S2, and DPC) produced no significant differences in the time constants; however, much smaller bin widths (20 ms, with steps of 10 ms) produced a rescaling of the time constants to smaller values (29, 68, 51, 93, 112, 118, 161, and 173 ms, respectively) but, importantly, maintained the core result of the temporal hierarchy of the somatosensory network.

timescales than S1 (areas 1 and 3b combined, $\tau = 67$ ms). Furthermore, the autocorrelation of areas 5 and 7b decay slower than those of all S1 subareas, with intermediate values between S1 and S2.

To complete the panorama, we performed the same measurements on S2 and DPC populations (Fig. 2*C*). We chose DPC

as an exemplary associative frontal area involved in this somatosensory task (3, 34, 37). These two higher-order areas, S2 ($\tau = 178$ ms) and DPC ($\tau = 182$ ms), display much larger decay constants, with values greater than those for all other areas analyzed in this work. This is further evidence that sensory information does not reverberate within the S1 network itself. As stated earlier, S1 exhibits a faster decay constant ($\tau = 67$ ms), with its constituent area 3b being the fastest ($\tau = 35$ ms). Despite comparable τ values in the S2 and DPC populations, the autocorrelation results for DPC start at and maintain higher values. This means that fluctuations do not reverberate equally within each area, despite approximately equivalent timescales. Furthermore, when a smaller bin width (20 ms, with steps of 10 ms) was used to calculate the autocorrelation function, the τ values from S2 and DPC exhibit a significant difference ($\tau = 161 \pm 4$ ms vs. 173 ± 3 ms); however, the intrinsic hierarchy remained. In *SI Appendix*, Fig. S1 *A–C*, we plot the same autocorrelation functions, including the SEM for each average value.

Hierarchical Timescales Are Invariant to Cognitive Demand. To what extent are these timescales dependent on the animal's behavioral report? Is the cortical hierarchy modified during the control task (LCT)? In a previous work, we observed a completely different effect of the LCT over neuronal activity depending on the cortical area (*SI Appendix*, Fig. S2). While neurons in area 3b (S1) did not alter their responses during the LCT (34, 35), DPC neurons stopped coding task parameters. Meanwhile, S2 neurons exhibited an intermediate duality of responses (*SI Appendix*); sensory neurons did not alter their dynamics, while categorical neurons ceased coding (31).

Surprisingly, all autocorrelation functions observed during the TPDT reappeared, unaffected, during the LCT (Fig. 3). The same hierarchical order was observed during this nondemanding control task. Even if some of the coding dynamics changed completely in S2 during the LCT and all coding dynamics disappeared in DPC (*SI Appendix*, Fig. S2), their autocorrelation functions did not change. These results provide further evidence that autocorrelation is a measure of an inherent feature of each cortical area of the network that does not depend on task context. *SI Appendix*, Fig. S1 *D* and *E* display these functions with SEM for comparison with the TPDT.

Timescales Are Intrinsic within Each Area. For each cortical area, neurons exhibit different types of dynamics during the TPDT. Focusing on area 1, it is possible to classify neurons depending on their receptive field. A high proportion of the recorded neurons exhibited receptive fields at the stimulated region ($n = 211$; 62.8%); however, approximately one-third of the recorded population was not stimulated in the receptive fields ($n = 125$; 37.2%). Given these electrophysiological differences, we wondered whether they affect the timescale properties that we observe. To test these results, we computed the autocorrelation in each subgroup (Fig. 4*A*). Notably, we observed analogous autocorrelation functions, with similar decay, for the whole area 1 population ($\tau = 84$ ms), as well as for neurons with receptive fields ($\tau = 77$ ms) and neurons without receptive fields ($\tau = 87$ ms). The autocorrelation decay functions depict a striking superposition. Thus, neurons with different receptive fields appear to be ingrained within the same somatosensory hierarchy.

Additionally, given that S2 neurons exhibit a high diversity of dynamics, ranging from pure sensory to pure categorical responses, we asked whether neurons exhibited different timescales depending on these dynamics. We selected subgroups of S2 neurons based on their dynamics using mutual information (38). We chose sensory neurons ($n = 105$) depending on their degree of phase locking to the stimulus pulses (*SI Appendix*). Furthermore, we identified categorical neurons with negligible sensory dynamic but strong categorical coding ($n = 150$; *SI Appendix*).
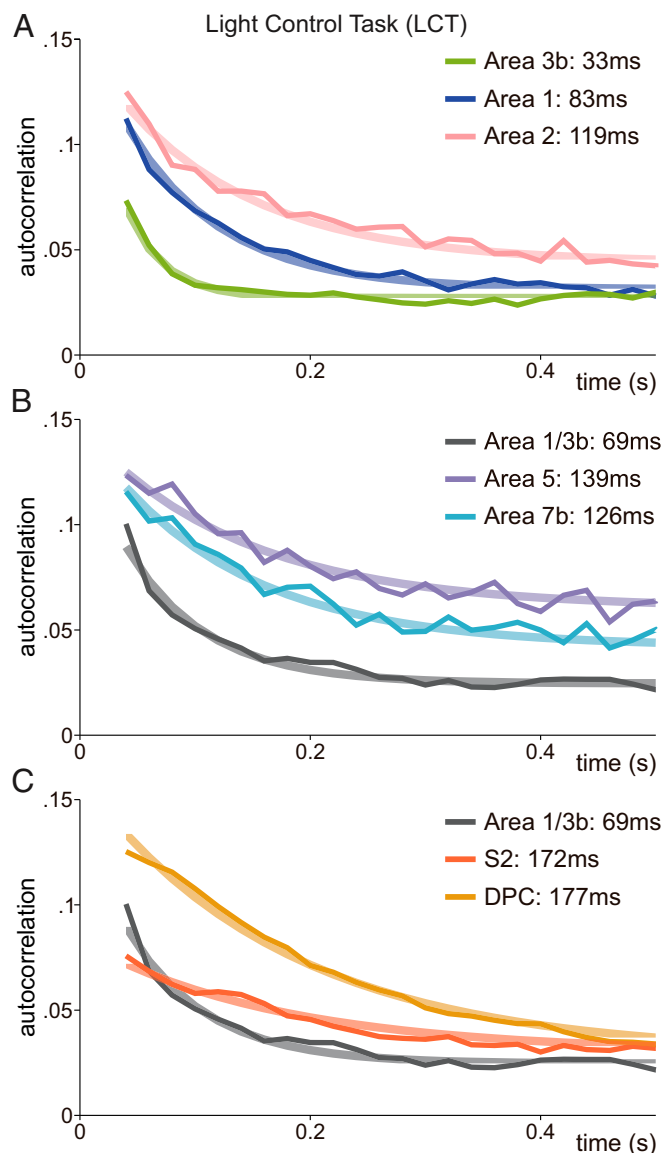
Rossi-Pool et al.
Invariant timescale hierarchy across the cortical somatosensory network

PNAS | 3 of 7
https://doi.org/10.1073/pnas.2021843118

Fig. 3. Hierarchical ordering of intrinsic timescales during the LCT. The autocorrelation function was computed for neuronal activity during the LCT basal period with 40-ms time bins. An exponential decay function was fit to the autocorrelation values (*SI Appendix*). Confidence intervals for τ were estimated with bootstrap. Thin, darker traces show the autocorrelation values averaged across each population of neurons. Wide, lighter traces display the exponential fit for each population. (*A*) LCT autocorrelation function for areas 3b (green; $n = 92$, $τ = 33 ± 12$ ms), 1 (blue; $n = 227$, $τ = 83 ± 16$ ms), and 2 (pink; $n = 23$, $τ = 119 ± 23$ ms). (*B*) Autocorrelation function for S1 (areas 3b and 1, gray; $n = 319$, $τ = 69 ± 10$ ms) compared with area 5 (violet, $n = 19$; $τ = 139 ± 27$ ms) and area 7b (cyan, $n = 32$; $τ = 126 ± 25$ ms). (*C*) LCT autocorrelation function for entire S1 (areas 3b and 1; gray) plotted against S2 (red; $n = 313$, $τ = 172 ± 15$ ms) and DPC (orange; $n = 462$, $τ = 177 ± 9$ ms) populations. Comparing Figs. 2 and 3 shows that for all areas, autocorrelation functions are analogous in TPDT and LCT.

Fig. 4*B* shows their corresponding autocorrelation functions. Surprisingly, we observed analogous autocorrelation functions, with similar decay rates, for sensory neurons ($τ = 182$ ms) and categorical neurons ($τ = 187$ ms), as well as for the whole S2 population ($τ = 178$ ms). Even if sensory and categorical neurons exhibit completely different coding dynamics, their autocorrelations show similar values (<3% difference). Although S2 subpopulations were engaged in different roles, they are fundamentally embedded within the same cortical hierarchy.
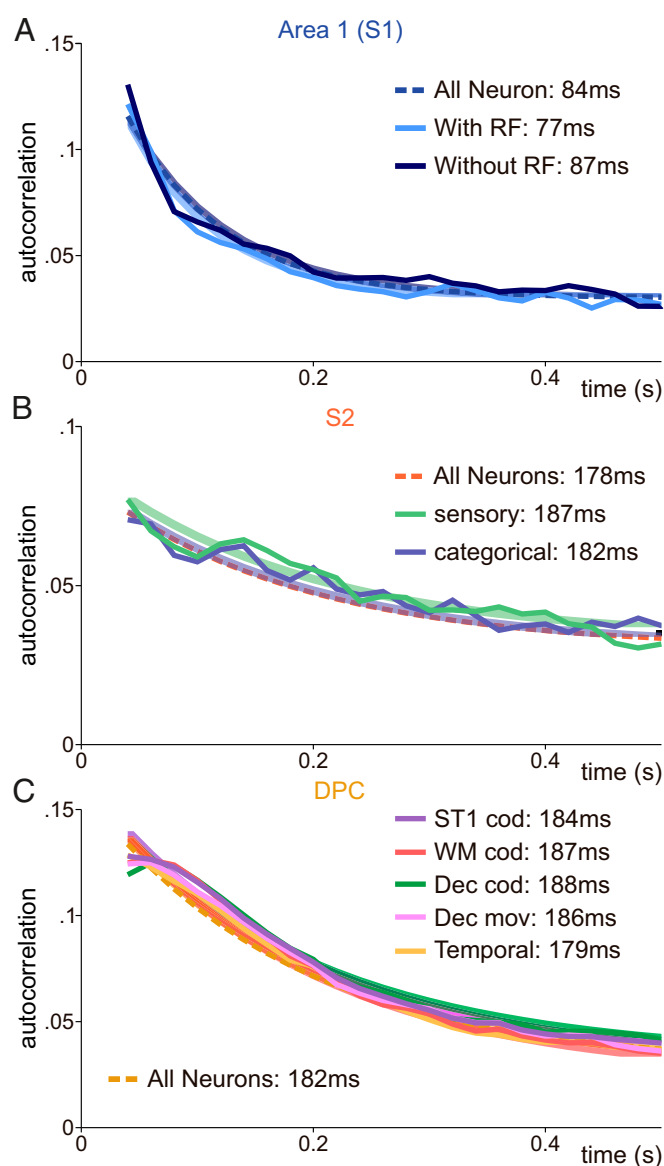
Fig. 4. Invariant intrinsic timescales across neural subgroups from the same area. The autocorrelation function was computed for neuronal activity of different subgroups of neurons during the TPDT basal period with 40-ms time bins. An exponential decay function was fit to the autocorrelation values (*SI Appendix*). Thin, darker traces show the autocorrelation values averaged across each group of neurons. Wide, lighter traces display the exponential fit for each subgroup. Dotted lines show the exponential decay fitted for all neurons from each area (same as Fig. 2). (*A*) TPDT autocorrelation function for two different subgroups of area 1 neurons with receptive field (light blue; $n = 211$, $τ = 77 ± 14$ ms) and without receptive field (dark blue; $n = 125$, $τ = 87 ± 15$ ms) compared with all area 1 neurons (blue dotted; $n = 336$, $τ = 84 ± 13$ ms). Autocorrelation is invariant for specific subgroups of area 1 neurons. (*B*) Autocorrelation function for the entire S2 population (red dotted; $n = 1,646$, $τ = 178 ± 10$ ms), the S2 sensory population (green; $n = 105$, $τ = 187 ± 16$ ms), and the S2 categorical population (blue; $n = 150$, $τ = 182 ± 14$ ms). Autocorrelation is invariant for S2 and its subpopulations. (*C*) TPDT autocorrelation function for different subgroups of DPC neurons: neurons with P1 coding during the first stimulus (violet; $n = 554$, $τ = 184 ± 8$ ms), neurons with P1 coding during the working memory period (red; $n = 346$, $τ = 187 ± 11$ ms), neurons with decision coding (green; $n = 314$, $τ = 188 ± 10$ ms), neurons with decision coding during movement (pink; $n = 386$, $τ = 186 ± 9$ ms), and neurons with pure temporal signals (orange; $n = 358$, $τ = 179 ± 12$ ms). The autocorrelation function for the entire DPC population is depicted for comparison (orange dotted; $n = 1,574$, $τ = 182 ± 5$ ms). Autocorrelation is invariant for specific subgroups of DPC neurons with different coding dynamics.

4 of 7 | PNAS
https://doi.org/10.1073/pnas.2021843118

Rossi-Pool et al.
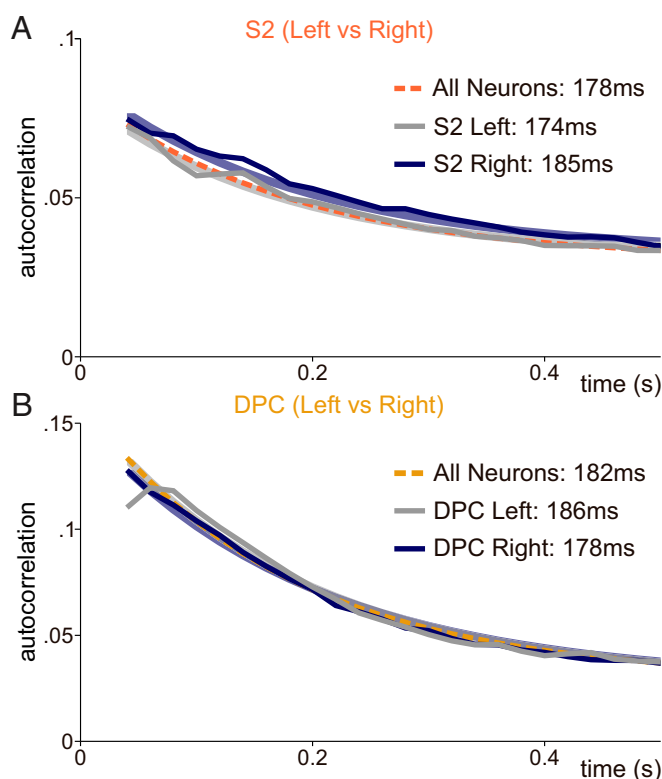Invariant timescale hierarchy across the cortical somatosensory network

Fig. 5. Invariant intrinsic timescales across the same area from different hemispheres. The autocorrelation function was computed for neuronal activity of neurons from different hemispheres during the TPDT basal period with 40 ms time bins. An exponential decay function was fit to the autocorrelation value (*SI Appendix*). Thin, darker traces show the autocorrelation values averaged across neurons from the same hemisphere. Wide, lighter traces display the exponential fit for each hemisphere. Dotted lines show the exponential decay fitted for all neurons from both hemispheres (same as Fig. 2). (*A*) TPDT autocorrelation function for neurons recorded in each hemisphere of S2: left hemisphere (gray; $n = 1,236$, $\tau = 174 \pm 11$ ms) and right hemisphere (dark blue; $n = 410$, $\tau = 185 \pm 14$ ms). The autocorrelation function for the entire S2 population is depicted for comparison (red dotted; $n = 1,646$, $\tau = 178 \pm 10$ ms). S2 autocorrelation is invariant across hemispheres. (*B*) Autocorrelation function for the entire DPC population (orange dotted; $n = 1,574$, $\tau = 182 \pm 5$ ms), the DPC left hemisphere population (gray; $n = 675$, $\tau = 186 \pm 8$ ms) or the DPC right hemisphere population (dark; $n = 899$, $\tau = 178 \pm 7$ ms). Autocorrelation is invariant between DPCs from different hemispheres.

We extended this analysis to subgroups of DPC neurons with different types of coding. In a previous work (34), we identified DPC neurons with mixed selectivity that code different task parameters during the TPDT. Here we split groups of DPC neurons depending on the parameters they coded and the time interval during which they were coded. Fig. 4*C* shows DPC neurons with significant P1 coding during the stimulation period (violet; $n = 554$, $\tau = 184$ ms), significant P1 coding during the working memory period (between P1 and P2; red; $n = 346$, $\tau = 187$ ms), decision coding during the comparison and postponed decision period (between P2 and probe up; green; $n = 314$, $\tau = 188$ ms), and decision coding during pushbutton movement (pink; $n = 386$, $\tau = 186$ ms), as well as neurons with pure temporal dynamics without coding (orange; $n = 358$, $\tau = 179$ ms). Remarkably, all autocorrelation functions behaved similarly irrespective of the type of neuron (Fig. 4*C*). Again, the functions exhibit a surprising superposition. These results are further evidence that timescales are an intrinsic measure of hierarchical

order in the somatosensory processing network, independent of the specific coding dynamics of each subgroup of neurons.

We remark that this inherent hierarchy is not comparable to a hierarchical order based on coding or response latencies (*SI Appendix*). In this case, neurons within each cortical area exhibit a broad distribution depending on their responses (*SI Appendix*, Fig. S3*A*). To show this, we split the S2 and DPC populations into subgroups based on their response latencies. The whole area distribution (S2 or DPC, *SI Appendix*, Fig. S3*A*) was divided into five groups (20% of width each). Then, for each curve in *SI Appendix*, Fig. S4, we pooled neurons with comparable latencies. While timescales do not depend on the single neuron responses, latencies are markedly dependent on them. Although DPC neurons depict a high diversity of responses that give rise to wide latency distributions, their autocorrelation is invariant to their dynamic (*SI Appendix*, Fig. S4*B*). *SI Appendix*, Fig. S3*A* displays the response and coding latency distributions for S2 sensory (green) and categorical neurons (blue). Again, while their latency distributions and mean values are completely different, their autocorrelation remains invariant (Fig. 4*A* and *SI Appendix*, Fig. S4*A*).

Same Hierarchical Order in Homologous Cortical Areas from Both Hemispheres. Finally, we divided S2 and DPC neurons according to their hemisphere. Note that these two cortical areas were the only areas recorded in both hemispheres (Fig. 1*C*). Importantly, during the TPDT, somatosensory information arrived to the cortex through the left hemisphere, and pushbutton movement was produced in the right hemisphere. Therefore, left and right areas may have different roles during this task. Based on this task characteristic, we investigated whether the autocorrelation function depends on the hemisphere (39). Notably, we obtained the same exponential decay for both left S2 ($\tau = 174$ ms) and right S2 ($\tau = 185$ ms) (Fig. 5*A*). Analogously, both DPCs depicted the same timescales (Fig. 5*B*) when we compared the autocorrelation functions between the left ($\tau = 186$ ms) and right hemispheres ($\tau = 178$ ms). These results suggest that homologous cortical areas at different hemispheres exhibit the same hierarchical order.

Discussion

Here we provide strong evidence that a hierarchical order in the cortical somatosensory network could be established by estimating an intrinsic timescale for each area. The timescale constant studied for this purpose was the exponential decay rate of the basal (resting state or foreperiod) autocorrelation. This time constant may play a relevant functional role in determining the period over which areas integrate their inputs. Primary sensory areas (3b and 1) display fast timescales and stimulus phase-locking responses, while S2 and DPC exhibit much longer time constants that are appropriate for integration. Importantly, we identified a clear difference in the timescale hierarchy among subareas 3b, 1, and 2 of S1. Furthermore, these intrinsic timescales are invariant within each area across both the TPDT and the LCT. Notably, the timescale persists for DPC neurons, although this area loses all significant coding during the LCT. Moreover, the same timescale was found for area 1, S2, and DPC across neuronal responses, regardless of their coding profiles. This suggests that this measure is intrinsic, indicative of a structural feature of each cortical area, and not a specific dynamic characteristic of each neuron.

The capacity of the cortex to integrate and maintain stimulus information in working memory is crucial for perceptual processes. At the same time, sensory areas in the cortex must be fast and locked to the stimuli. Owing to these conflicting needs, the brain requires a diversity of coexisting timescales during cognitive processes. In this case, long time constants could facilitate the first set of cortical computations that depend on signal integration or maintenance. Nevertheless, long time constants would interfere with the faithful representation of stimuli; thus,

Rossi-Pool et al.
Invariant timescale hierarchy across the cortical somatosensory network

PNAS | 5 of 7
https://doi.org/10.1073/pnas.2021843118

shorter time constants are still necessary. This might provide a connection between function and structural heterogeneities.

In general, a hierarchy should be independent of the specific cognitive task studied. Consider, for instance, a pair of areas that have converged to the same signals for a task but are known to have different positions within a hierarchy. The trait by which these areas were sorted in the hierarchy should still reflect the difference between them, even if their signals or functions appear to be the same for a specific task. However, the inverse is not necessarily true. A pair of cortical areas that produce different signals need not be sharply distinct in their hierarchical position. Both cases might be at play in our results. Thus, the correspondence between functional roles and hierarchical position is not one-to-one.

Surprisingly, we identify a stratification inside the three sub-areas that constitute S1. Area 1 is able to integrate temporal information with a much longer time constant than area 3b. Even if differences in periodicity exist between neurons from areas 1 and 3b during the vibrotactile discrimination task (13), their firing rate responses are analogous. However, to our knowledge, there is no cognitive task designed to compare responses between these two areas. A possible hypothesis is that noticeable firing rate differences will emerge between these areas during cognitive tasks where temporal integration is mandatory. Importantly, the time constant of areas downstream to area 1 (areas 2, 5, 7b, and S2) depict much longer values, >110 ms. It was previously found that the optimal integration window for decoding stimulus identity from neurons from area 3b was >150 ms (34, 40). In particular, this value agrees with the timescale found here for S2, which is crucial for sensory integration (13, 31, 41, 42).

Although strongly related to both anatomy and function, the evidence from the analysis used here is neither anatomical nor functional. This follows from the ideas presented previously: area 1 and 3b are anatomically similar but distinct in their timescales, and S2 and DPC have signals that suggest very different functions but share similar autocorrelation decay timescales. In both cases, considering the relationship among these three perspectives (anatomy, function, and dynamics) leads to new hypotheses. Anatomy could structure these dynamic constants, which then in turn allow certain functions to arise. In this sense, dynamic features like time constants enable function.

Additionally, we explored this timescale hierarchical order during a cognitively nondemanding control task, the LCT. While a passive control used in previous studies eliminated the motor report of the task (37), the LCT still requires the monkey to report a decision, indicated instead by an illuminated pushbutton (34). Remarkably, the timescales remained invariant within each area during both the TPDT and LCT. During LCT, S2 neurons exhibit only sensory dynamics, with no categorical responses (31). Furthermore, this constant timescale persists for DPC neurons despite losing all significant coding during the LCT. Then, even if categorical coding and heterogeneous dynamics were to cease in several cortical areas during LCT, their inherent timescales would remain. This is an important control that supports the hypothesis that cortical areas exhibit a structural and invariant hierarchical order depending on functionality (1).

Notably, although neurons of S2 and DPC display a vast diversity of dynamic coding, we found no relationship between their specific neuronal responses and their time constants. Even when we chose extreme neurons at each cortical population, their autocorrelation function behaved as the whole network. Moreover, we did not identify differences across hemispheres. Furthermore, neurons in area 1 with and without receptive fields displayed similar temporal constants. Our results provide more evidence that time constants may indicate a fundamental organizational feature for network processing at each cortical area. The data suggest that this intrinsic timescale does not correlate to single neuron coding or physiology but rather is a macroscopic

feature of each cortical area. Importantly, other studies focusing on reward time constants found an analogous hierarchy in the visual pathway (10, 36, 43); however, controversy has emerged based on research supporting independence between coding and time constants (10) and other studies suggesting that the decay constant can be used to predict single neuron coding (36, 44). More studies and experiments are needed to analyze in detail the heterogeneity of single neuron timescales at each cortical area.

In recent years, the heterogeneous responses from several cognitive tasks have been analyzed with dimensionality reduction techniques to condense the dynamics into the relevant population signals (3, 35, 45). Importantly, the network's dynamics could be described with a small number of significant dimensions (46–48). However, whether dimensionality increases with hierarchical cortical order remains an open question. A recent work has shown that the number of significant dimensions increases from V1 to V2 (49), but whether this is a general principle across cortices is unclear. Future studies should analyze in detail the relationship between timescale hierarchies and dimensions. However, it is important to note that although the timescales do not change during the nondemanding task, dimensionality is reduced (50). Thus, while dimensionality is a dynamic feature that depends on task requirements, timescale hierarchy is invariant.

Which network properties generate the time constant gradient found here remains an open question. A possible physiological factor that may account for part of this hierarchy is the recurrent connectivity within each cortical area. These recurrent synapses represent 80% of all excitatory connections (51). Furthermore, research has shown a positive correlation between recurrent excitatory connections, measured with spine counts, and the hierarchical position of each area (4). Some models have used this organizational principle to explain persistent working memory responses through bifurcations in the network dynamics (1, 17). Moreover, a recent computational model (4) has shown evidence that this temporal organization may emerge from weighted connectivity (51). In that study, the authors analyzed the time constant during stimulation. Even though this dynamic timescale may be different from the resting state time constant studied, it shows that heterogeneity in connectivity may explain temporal hierarchy. Based on that result, a reevaluation of studies that assume equality between cortical areas to compute functional connectivity is mandatory (1, 4).

We would like to highlight that the inherent hierarchy found here is not associated with the response latency organization observed in the somatosensory network during stimulation (27, 37). The time constant studied here is more pertinently viewed as a structural feature of each cortical node. Even the DPC population without any coding during LCT exhibits this inherent feature. Furthermore, while S2 sensory and categorical neurons depict completely different signals during stimulation, they possess the same autocorrelation decay. The stratification of structural and invariant time constants across the somatosensory network appears to be a general organizational principle. The diversity of structural characteristics among cortical nodes may be crucial to understanding brain function and computations during cognitive processes.

Materials and Methods

Monkeys were trained to report whether the temporal structure of two vibrotactile stimuli of equal frequency was the same or different (*SI Appendix*). Neuronal recordings were obtained in cortical areas while the monkeys performed the TPDT. Animals were handled in accordance with standards of the National Institutes of Health and Society for Neuroscience. All protocols were approved by the Institutional Animal Care and Use Committee of the Instituto de Fisiología Celular, Universidad Nacional Autónoma de México.

Data Availability. Data files are publicly available at Zenodo (DOI: 10.5281/zenodo.4421855); see reference (52).

6 of 7 | PNAS
https://doi.org/10.1073/pnas.2021843118

Rossi-Pool et al.
Invariant timescale hierarchy across the cortical somatosensory network

1. X.-J. Wang, Macroscopic gradients of synaptic excitation and inhibition in the neocortex. *Nat. Rev. Neurosci.* **21**, 169–178 (2020).
2. K. Wagstyl, L. Ronan, I. M. Goodyer, P. C. Fletcher, Cortical thickness gradients in structural hierarchies. *Neuroimage* **111**, 241–250 (2015).
3. R. Romo, R. Rossi-Pool, Turning touch into perception. *Neuron* **105**, 16–33 (2020).
4. R. Chaudhuri, K. Knoblauch, M.-A. Gariel, H. Kennedy, X.-J. Wang, A large-scale circuit mechanism for hierarchical dynamical processing in the primate cortex. *Neuron* **88**, 419–431 (2015).
5. M. R. Joglekar, J. F. Mejias, G. R. Yang, X.-J. Wang, Inter-areal balanced amplification enhances signal propagation in a large-scale circuit model of the primate cortex. *Neuron* **98**, 222–234.e8 (2018).
6. A. Anticevic, J. Lisman, How can global alteration of excitation/inhibition balance lead to the local dysfunctions that underlie schizophrenia? *Biol. Psychiatry* **81**, 818–820 (2017).
7. G. D. Hoftman *et al.*, Altered gradients of glutamate and gamma-aminobutyric acid transcripts in the cortical visuospatial working memory network in schizophrenia. *Biol. Psychiatry* **83**, 670–679 (2018).
8. J. D. Murray *et al.*, A hierarchy of intrinsic timescales across primate cortex. *Nat. Neurosci.* **17**, 1661–1663 (2014).
9. J. H. Siegle *et al.*, A survey of spiking activity reveals a functional hierarchy of mouse corticothalamic visual areas. *bioRxiv*, https://doi.org/10.1101/805010 (2019).
10. M. Spitmaan, H. Seo, D. Lee, A. Soltani, Multiple timescales of neural dynamics and integration of task-relevant signals across cortex. *Proc. Natl. Acad. Sci. U.S.A.* **117**, 22522–22531 (2020).
11. U. Hasson, E. Yang, I. Vallines, D. J. Heeger, N. Rubin, A hierarchy of temporal receptive windows in human cortex. *J. Neurosci.* **28**, 2539–2550 (2008).
12. C. J. Honey *et al.*, Slow cortical dynamics and the accumulation of information over long timescales. *Neuron* **76**, 423–434 (2012).
13. E. Salinas, A. Hernández, A. Zainos, R. Romo, Periodicity and firing rate as candidate neural codes for the frequency of vibrotactile stimuli. *J. Neurosci.* **20**, 5503–5515 (2000).
14. J. H. R. Maunsell, W. T. Newsome, Visual processing in monkey extrastriate cortex. *Annu. Rev. Neurosci.* **10**, 363–401 (1987).
15. D. J. Felleman, D. C. Van Essen, Distributed hierarchical processing in the primate cerebral cortex. *Cereb. Cortex* **1**, 1–47 (1991).
16. X.-J. Wang, Probabilistic decision making by slow reverberation in cortical circuits. *Neuron* **36**, 955–968 (2002).
17. X. J. Wang, Synaptic reverberation underlying mnemonic persistent activity. *Trends Neurosci.* **24**, 455–463 (2001).
18. E. Pálfi *et al.*, Connectivity of neuronal populations within and between areas of primate somatosensory cortex. *Brain Struct. Funct.* **223**, 2949–2971 (2018).
19. N. Saadon-Grosman, S. Arzy, Y. Loewenstein, Hierarchical cortical gradients in somatosensory processing. *Neuroimage* **222**, 117257 (2020).
20. W. H. Talbot, I. Darian-Smith, H. H. Kornhuber, V. B. Mountcastle, The sense of flutter-vibration: Comparison of the human capacity with response patterns of mechanoreceptive afferents from the monkey hand. *J. Neurophysiol.* **31**, 301–334 (1968).
21. P. R. Douglas, D. G. Ferrington, M. Rowe, Coding of information about tactile stimuli by neurones of the cuneate nucleus. *J. Physiol.* **285**, 493–513 (1978).
22. L. Camarillo, R. Luna, V. Nácher, R. Romo, Coding perceptual discrimination in the somatosensory thalamus. *Proc. Natl. Acad. Sci. U.S.A.* **109**, 21093–21098 (2012).
23. V. B. Mountcastle, W. H. Talbot, H. Sakata, J. Hyvärinen, Cortical neuronal mechanisms in flutter-vibration studied in unanesthetized monkeys: Neuronal periodicity and frequency discrimination. *J. Neurophysiol.* **32**, 452–484 (1969).
24. M. Ashaber *et al.*, Connectivity of somatosensory cortical area 1 forms an anatomical substrate for the emergence of multifinger receptive fields and complex feature selectivity in the squirrel monkey (Saimiri sciureus). *J. Comp. Neurol.* **522**, 1769–1785 (2014).
25. A. Hernández, A. Zainos, R. Romo, Neuronal correlates of sensory discrimination in the somatosensory cortex. *Proc. Natl. Acad. Sci. U.S.A.* **97**, 6191–6196 (2000).
26. L. Lemus, A. Hernández, R. Luna, A. Zainos, R. Romo, Do sensory cortices process more than one sensory modality during perceptual judgments? *Neuron* **67**, 335–348 (2010).
27. V. de Lafuente, R. Romo, Neural correlate of subjective sensory experience gradually builds up across cortical areas. *Proc. Natl. Acad. Sci. U.S.A.* **103**, 14266–14271 (2006).
28. C. Cavada, P. S. Goldman-Rakic, Posterior parietal cortex in rhesus monkey: I. Parcellation of areas based on distinctive limbic and sensory corticocortical connections. *J. Comp. Neurol.* **287**, 393–421 (1989).
29. M. K. L. Baldwin, D. F. Cooke, A. B. Goldring, L. Krubitzer, Representations of fine digit movements in posterior and anterior parietal cortex revealed using long-train intracortical microstimulation in macaque monkeys. *Cereb. Cortex* **28**, 4244–4263 (2018).
30. R. Romo, A. Hernández, A. Zainos, L. Lemus, C. D. Brody, Neuronal correlates of decision-making in secondary somatosensory cortex. *Nat. Neurosci.* **5**, 1217–1225 (2002).
31. R. Rossi-Pool, A. Zainos, M. Alvarez, G. D. Leon, R. Romo, From an invariant sensory code to a perceptual categorical code in secondary somatosensory cortex. *bioRxiv*, https://doi.org/10.1101/2020.03.31.018879 (2020).
32. R. Romo, E. Salinas, Flutter discrimination: Neural codes, perception, memory and decision making. *Nat. Rev. Neurosci.* **4**, 203–218 (2003).
33. R. Rossi-Pool, J. Vergara, R. Romo, "Constructing perceptual decision-making across cortex" in *The Cognitive Neurosciences, 6/E*, D. Poeppel, G. Mangun, M. Gazzaniga, Eds. (The MIT Press, 2020), pp. 413–427.
34. R. Rossi-Pool *et al.*, Emergence of an abstract categorical code enabling the discrimination of temporally structured tactile stimuli. *Proc. Natl. Acad. Sci. U.S.A.* **113**, E7966–E7975 (2016).
35. R. Rossi-Pool *et al.*, Decoding a decision process in the neuronal population of dorsal premotor cortex. *Neuron* **96**, 1432–1446.e7 (2017).
36. S. E. Cavanagh, J. D. Wallis, S. W. Kennerley, L. T. Hunt, Autocorrelation structure at rest predicts value correlates of single neurons during reward-guided choice. *eLife* **5**, e18937 (2016).
37. A. Hernández *et al.*, Decoding a perceptual decision process across cortex. *Neuron* **66**, 300–314 (2010).
38. S. Panzeri, R. Senatore, M. A. Montemurro, R. S. Petersen, Correcting for the sampling bias problem in spike train information measures. *J. Neurophysiol.* **98**, 1064–1072 (2007).
39. I. Kagan, A. Iyer, A. Lindner, R. A. Andersen, Space representation for eye movements is more contralateral in monkeys than in humans. *Proc. Natl. Acad. Sci. U.S.A.* **107**, 7933–7938 (2010).
40. R. Luna, A. Hernández, C. D. Brody, R. Romo, Neural codes for perceptual discrimination in primary somatosensory cortex. *Nat. Neurosci.* **8**, 1210–1219 (2005).
41. R. V. Bretas, M. Taoka, H. Suzuki, A. Iriki, Secondary somatosensory cortex of primates: Beyond body maps, toward conscious self-in-the-world maps. *Exp. Brain Res.* **238**, 259–272 (2020).
42. C. Condylis *et al.*, Context-dependent sensory processing across primary and secondary somatosensory cortex. *Neuron* **106**, 515–525.e5 (2020).
43. A. Bernacchia, H. Seo, D. Lee, X.-J. Wang, A reservoir of time constants for memory traces in cortical neurons. *Nat. Neurosci.* **14**, 366–372 (2011).
44. D. F. Wasmuht, E. Spaak, T. J. Buschman, E. K. Miller, M. G. Stokes, Intrinsic neuronal dynamics predict distinct functional roles during working memory. *Nat. Commun.* **9**, 3499 (2018).
45. F. Carnevale, V. de Lafuente, R. Romo, O. Barak, N. Parga, Dynamic control of response criterion in premotor cortex during perceptual detection under temporal uncertainty. *Neuron* **86**, 1067–1077 (2015).
46. E. M. Trautmann *et al.*, Accurate estimation of neural population dynamics without spike sorting. *Neuron* **103**, 292–308.e4 (2019).
47. P. Gao, S. Ganguli, On simplicity and complexity in the brave new world of large-scale neuroscience. *Curr. Opin. Neurobiol.* **32**, 148–155 (2015).
48. R. Rossi-Pool, R. Romo, Low dimensionality, high robustness in neural population dynamics. *Neuron* **103**, 177–179 (2019).
49. J. D. Semedo, A. Zandvakili, C. K. Machens, B. M. Yu, A. Kohn, Cortical areas interact through a communication subspace. *Neuron* **102**, 249–259.e4 (2019).
50. R. Rossi-Pool *et al.*, Temporal signals underlying a cognitive process in the dorsal premotor cortex. *Proc. Natl. Acad. Sci. U.S.A.* **116**, 7523–7532 (2019).
51. N. T. Markov *et al.*, A weighted and directed interareal connectivity matrix for macaque cerebral cortex. *Cereb. Cortex* **24**, 17–36 (2014).
52. A. Zainos *et al*, "Single Neuron Activity of S1, S2 and DPC of Macaca Mulatta Subjects performing the Temporal Pattern Discrimination Task." *Zenodo.* 10.5281/zenodo.4421855. Deposited 6 January 2021.

Rossi-Pool et al.
Invariant timescale hierarchy across the cortical somatosensory network

PNAS | 7 of 7
https://doi.org/10.1073/pnas.2021843118